

## Assessment of local influence for the analysis of agreement

Carla Leal <sup>1</sup>, Manuel Galea <sup>2</sup>, and Felipe Osorio\*.<sup>3</sup>

<sup>1</sup> Centro Regional de Inclusión e Innovación Social, Universidad Viña del Mar, Diego Portales 90, Viña del Mar, Chile.

<sup>2</sup> Departamento de Estadística, Pontificia Universidad Católica de Chile, Av. Vicuña Mackenna 4860, Santiago, Chile.

<sup>3</sup> Departamento de Matemática, Universidad Técnica Federico Santa María, Av. España 1680, Valparaíso, Chile.

Received 7 May 2018, revised 24 October 2018, accepted 19 December 2018

The concordance correlation coefficient (CCC) and the probability of agreement (PA) are two frequently used measures for evaluating the degree of agreement between measurements generated by two different methods. In this paper, we consider the CCC and the PA using the bivariate normal distribution for modeling the observations obtained by two measurement methods. The main aim of this paper is to develop diagnostic tools for the detection of those observations that are influential on the maximum likelihood estimators of the CCC and the PA using the local influence methodology but not based on the likelihood displacement. Thus, we derive first- and second-order measures considering the case-weight perturbation scheme. The proposed methodology is illustrated through a Monte Carlo simulation study and using a dataset from a clinical study on transient sleep disorder. Empirical results suggest that under certain circumstances first-order local influence measures may be more powerful than second-order measures for the detection of influential observations.

*Key words:* Concordance correlation coefficient; First- and second-order approaches; normal and conformal curvatures; Probability of agreement

### 1 Introduction

To assess the degree of agreement between measurements obtained from two measurement instruments (or methods), [Lin \(1989\)](#) proposed a scaled index called the concordance correlation coefficient. This coefficient has been constructed to quantify the proximity of the measurements generated by the instruments to the 45° line passing through the origin, also known as the concordance line. The coefficient can be decomposed into two main components, the first quantifying how far each observation moves from the line that represents the best fit to the data (precision) and the second measuring how far this fitted line deviates from the 45° line (accuracy). The need to measure the agreement between measurement instruments frequently arises in several areas of knowledge; see for instance [Carstensen \(2010\)](#), [Lin et al. \(2011\)](#) and [Choudhary and Nagaraja \(2017\)](#). Recent works proposing a version of the CCC to manipulate several measuring instruments as well as a technique to evaluate the agreement between two instruments that leads to an interesting graphic tool are described by [Hiriote and Chinchilli \(2011\)](#) and [Stevens et al. \(2017\)](#), respectively. We can use other measures of agreement. In this paper we consider also the probability of agreement, suggested by [Stevens et al. \(2017\)](#) and [Choudhary and Nagaraja \(2017\)](#).

[Cook \(1986\)](#) proposed a general diagnostic procedure to study the sensitivity of certain statistics of interest when minor perturbations to model assumptions and/or data are introduced on the postulated statistical model through the evaluation of the local behavior of some influence measure. In particular, [Cook \(1986\)](#) suggested assessing the effect of a particular perturbation scheme by investigating the behavior of

---

\*Corresponding author: e-mail: felipe.osorios@usm.cl, Phone: +56-32-265 4153

the surface generated by the likelihood displacement. However, we are frequently interested in the detection of potentially influential observations on a function of the maximum likelihood (ML) estimator. First-order local influence approaches applied to objective functions other than the likelihood displacement have been proposed, for instance, by [Lawrance \(1988\)](#), [Thomas and Cook \(1990\)](#) and [Cadigan and Farrel \(2002\)](#). Some authors have warned about the use of these procedures. For instance, [Wu and Luo \(1993\)](#) emphasized that first-order local influence does not always provide information on those observations that strongly influence objective functions defined as functions of the ML estimator. Moreover, [Fung and Kwan \(1997\)](#) showed that the normal curvature is not well defined for objective functions with non-zero first derivatives at the critical point, which can lead to misleading interpretations about the role of influential observations. To prevent these adverse effects, [Zhu et al. \(2007\)](#) proposed influence measures applicable to any differentiable objective function, regardless of whether its first derivative at the critical point is zero. They called these procedures first- and second-order approaches. The methodology has been applied by several authors. For example, [Chen et al. \(2009\)](#) developed the second-order local influence for nonlinear structural equation models, whereas [Shi et al. \(2009\)](#) studied the selection of appropriate perturbation schemes and proposed several first-order influence measures. Recently, [Giménez and Galea \(2013\)](#) and [Galea and Giménez \(2016\)](#) discussed the application of second-order approaches to assessing local influence in functional heteroscedastic measurement error models and the test of mean-variance efficiency in the capital asset pricing model, respectively. The application of this methodology to CCC and PA has not been previously considered in the literature.

The paper is organized as follows. In Section 2, we review the concordance correlation coefficient and the probability of agreement and introduce a dataset from a clinical study that will serve as a motivating example. Section 3 is dedicated to the development of the local influence for the CCC and the probability of agreement considering both first- and second-order measures under the case-weight perturbation scheme. Numerical experiments, based on a simulation study and the analysis of the motivating example, are presented in Sections 4 and 5, respectively. Finally, Section 6 gives some concluding remarks.

## 2 Some agreement measures

Let us assume a random sample  $(X_{11}, X_{12}), \dots, (X_{n1}, X_{n2})$  from a bivariate population with mean vector  $\boldsymbol{\mu}$  and covariance matrix  $\boldsymbol{\Sigma}$ . Then, a method to quantify the degree of agreement between the variables  $X_1$  and  $X_2$  corresponds to the CCC ([Lin, 1989](#)), which is defined as

$$\rho_c = \frac{2\sigma_{12}}{\sigma_{11} + \sigma_{22} + (\mu_1 - \mu_2)^2}, \quad (1)$$

where  $\mu_j$  and  $\sigma_{jj}$  are the mean and variance of the measurements obtained by the  $j$ th method or instrument of measurement, respectively ( $j = 1, 2$ ), and  $\sigma_{12}$  is the covariance between the measurements from methods 1 and 2. It is easy to see that the CCC can be written as a function of the precision and accuracy coefficients. Indeed,  $\rho_c = \rho_{12}C_{12}$ , where  $\rho_{12}$  shows how far each observation deviates from the best-fit line and  $C_{12} = 2(b + b^{-1} + a^2)^{-1}$  is a correction factor that measures how far the best-fit line deviates from the  $45^\circ$  line, in which  $b = (\sigma_{11}/\sigma_{22})^{1/2}$  and  $a = (\mu_1 - \mu_2)/(\sigma_{11}\sigma_{22})^{1/4}$ . Moreover, it is possible to show that the CCC is between  $-1$  and  $1$ , and a higher absolute value indicates a greater agreement between the measurements. Let  $D_i = X_{i1} - X_{i2}$  for  $i = 1, \dots, n$ , be the differences between the measurements obtained by the two instruments. Therefore, in order to quantify the degree of agreement between two systems of measurement [Stevens et al. \(2017\)](#) introduced the probability of agreement defined as

$$\psi_c = P(|D_i| \leq c), \quad c > 0,$$

where  $CAD = (-c, c)$  represents a clinically acceptable difference. In addition, we are assuming that the observations  $(X_{i1}, X_{i2})$ ,  $i = 1, \dots, n$ , were selected from a bivariate normal population. Thus, the

probability of agreement assumes the form

$$\psi_c = \Phi\left(\frac{c - \mu_D}{\sigma_D}\right) - \Phi\left(-\frac{c - \mu_D}{\sigma_D}\right), \quad (2)$$

where  $\Phi(\cdot)$  denotes the cumulative distribution function of the standard normal, and  $\mu_D = \mu_1 - \mu_2$ ,  $\sigma_D^2 = \sigma_{11} + \sigma_{22} - 2\sigma_{12}$ . Based on the normality assumption, the postulated statistical model is given by  $\mathcal{P} = \{p(\mathbf{x}; \boldsymbol{\theta}) : \boldsymbol{\theta} \in \Theta\}$ . In such case, the likelihood function can be written as

$$L(\boldsymbol{\theta}) = \prod_{i=1}^n \left[ (2\pi)^{-d/2} |\boldsymbol{\Sigma}|^{-1/2} \exp \left\{ -\frac{1}{2} (\mathbf{x}_i - \boldsymbol{\mu})^\top \boldsymbol{\Sigma}^{-1} (\mathbf{x}_i - \boldsymbol{\mu}) \right\} \right], \quad (3)$$

where  $\boldsymbol{\theta} = (\boldsymbol{\mu}^\top, \boldsymbol{\phi}^\top)^\top \in \mathbb{R}^{d(d+3)/2}$ ; in our case,  $d = 2$ , with  $\boldsymbol{\phi} = \text{vech}(\boldsymbol{\Sigma})$  and the  $\text{vech}(\cdot)$  operator defined in Magnus and Neudecker (2007, Sec. 3.8). The log-likelihood for (3) is  $\ell(\boldsymbol{\theta}) = \sum_{i=1}^n \ell_i(\boldsymbol{\theta})$ , where

$$\ell_i(\boldsymbol{\theta}) = -\frac{d}{2} \log(2\pi) - \frac{1}{2} \log |\boldsymbol{\Sigma}| - \frac{1}{2} (\mathbf{x}_i - \boldsymbol{\mu})^\top \boldsymbol{\Sigma}^{-1} (\mathbf{x}_i - \boldsymbol{\mu}). \quad (4)$$

The maximum likelihood estimation of  $\boldsymbol{\mu}$  and  $\boldsymbol{\Sigma}$  is described, for instance, in Anderson (2003, Sec. 3.2). Thus, substituting these ML estimates into Equations (1) and (2), we arrive at the ML estimates  $\hat{\rho}_c$  and  $\hat{\psi}_c$ . It should be stressed that under mild assumptions, Lin (1989) derived the asymptotic distribution for  $\hat{\rho}_c$ , allowing one to address the statistical inference and enabling, for instance, the construction of confidence intervals. Details regarding the calculation of the asymptotic distribution for  $\hat{\psi}_c$  are deferred to Appendix A.

## 2.1 Motivating example

Svetnik et al. (2007) conducted a clinical study designed to compare the automated and semi-automated scoring of Polysomnographic (PSG) recordings used to diagnose transient sleep disorders. The study considered 82 patients who were given a sleep-inducing drug (Zolpidem 10 mg). Measurements of latency to persistent sleep (LPS: lights out to the beginning of 10 consecutive minutes of uninterrupted sleep) were obtained using six different methods. In this work, we focus on two of these methods: fully manual scoring (Manual) and automated scoring by the Morpheus software (Automatic). Let  $\mathbf{X}_i = (X_{i1}, X_{i2})^\top$ , for  $i = 1, \dots, 82$ , be the log(LPS) measurements obtained with the manual and automatic methods, respectively. The measurements have quite similar behavior, and their differences present a slight asymmetry with some extreme observations (see Figure 1c)

The moment estimates for the mean vector and covariance matrix are

$$\bar{\mathbf{x}} = \begin{pmatrix} 2.554 \\ 2.309 \end{pmatrix}, \quad \mathbf{S} = \begin{pmatrix} 0.771 & 0.703 \\ 0.703 & 1.252 \end{pmatrix}.$$

Thus, the estimated generalized variance is  $\det(\mathbf{S}) = 0.472$ , showing that dispersion of the dataset is not large, although the precision coefficient is something low ( $\hat{\rho}_{12} = 0.715$ ). The sample estimator for the CCC is 0.675, which is close to the 0.650 cut-off proposed by McBride (2005), suggesting a low degree of agreement between the log(LPS) measurements. One explanation for this phenomenon is that there are some observations far from the concordance line. Indeed, Figure 1a shows that cases 1, 30 and 79 move away from the concordance line, and Figure 1b reveals that these observations lead to a lack of agreement because they are off-limits. It is interesting to note that if subjects 1, 30 and 79 are eliminated from the dataset, the sample estimate of the CCC becomes 0.860 ( $\hat{C}_{12} = 0.967$  and  $\hat{\rho}_{12} = 0.889$ ); the degree of agreement is increased by 28% mainly due to an increase in the precision coefficient. We must however stress that the coefficient of accuracy is not strongly affected. We can see an analogous effect

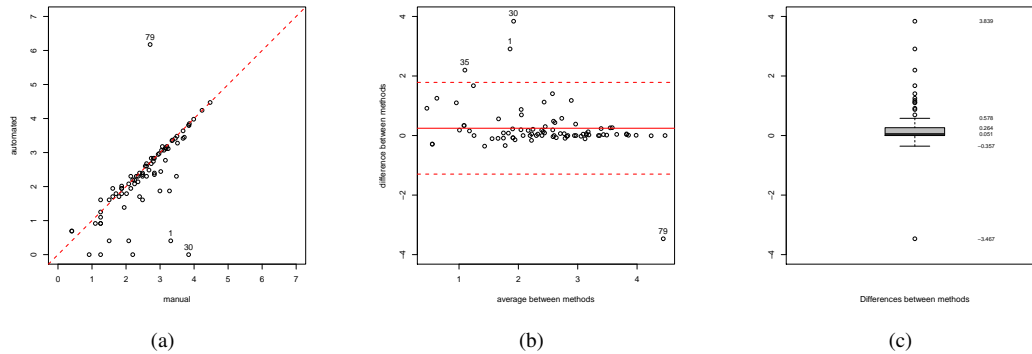


**Figure 1** Comparison of the two measurement methods (a), averages versus differences between manual and automatic methods (b) and boxplot of the differences between the measurement methods (c)

**Table 1** Estimates of CCC (standard errors in parenthesis), precision and accuracy and 95% asymptotic confidence interval

	CCC	Precision	Accuracy	Confidence Interval
With all subjects	0.674 (0.056)	0.715	0.943	(0.564, 0.785)
Subjects 1,30,79 removed	0.860 (0.028)	0.890	0.967	(0.806, 0.915)

**Table 2** Estimates of the probability of agreement ( $c = 2$ ), standard error and 95% asymptotic confidence interval

	$\psi_c$	SE	Confidence Interval
With all subjects	0.975	0.034	(0.909, 1.000)
Subjects 1,30,79 removed	0.999	0.001	(0.998, 1.000)

on the probability of agreement when observations 1, 30 and 79 are removed from the dataset, in all our experiments we have used  $c = 2$ , which in practice must be fixed by the data analyst or based on clinical judgment.

Figure 2 reveals that by removing subjects 1, 30 and 79, the agreement between measurements increases by 6%, 10% and 7%, respectively, whereas when deleting the remaining subjects, the agreement between the log(LPS) measurements remains between 0.657 and 0.691 (the dashed line denotes the CCC estimate with all observations included). Hence, we can notice that the estimator of the CCC is sensitive to the deletion of observations 1, 30 and 79, either individually or simultaneously (compare with Table 1). It should be noted that, although the estimator of  $\psi_c$  is sensitive to the presence of observations 1, 30 and 79, its influence in percentual terms seems to be lower. In the sequel, we develop local influence techniques to detect cases that are potentially influential on the estimators of the CCC and the probability of agreement,  $\psi_c$ . A remarkable feature of the proposed procedure is its ability to evaluate the simultaneous effects of influential observations without the need to remove such observations from the dataset.

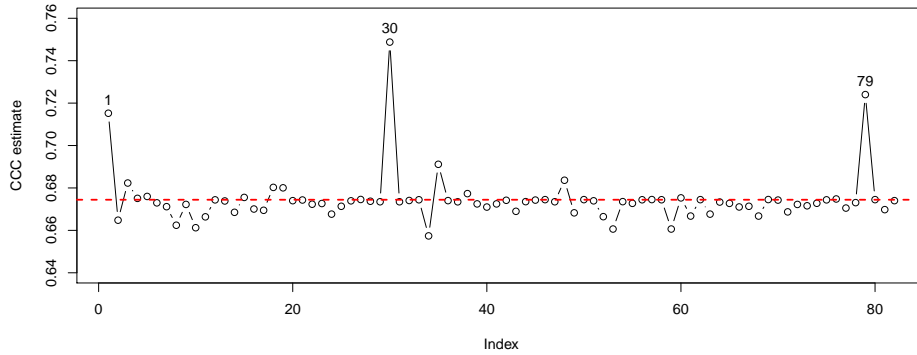


**Figure 2** Case deletion plot: CCC estimates when the  $i$ th observation have been removed from the dataset.

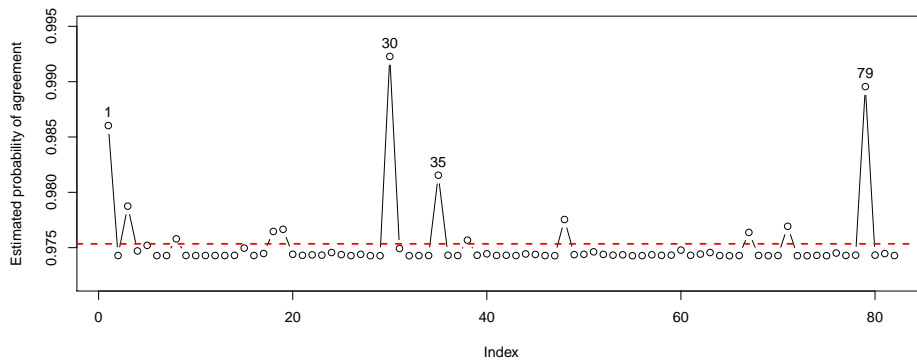


**Figure 3** Case deletion plot:  $\psi_c$  estimates when the  $i$ th observation have been removed from the dataset.

### 3 Influence diagnostics for measures of agreement

#### 3.1 Background

To assess the influence of extreme observations on the maximum likelihood estimates, [Cook \(1986\)](#) proposed to study the curvature of a particular influence measure based on the likelihood function. Indeed, his work used the likelihood displacement

$$LD(\omega) = 2\{\ell(\hat{\theta}) - \ell(\hat{\theta}(\omega))\}, \tag{5}$$

where  $\hat{\theta}$  and  $\hat{\theta}(\omega)$  are the maximum likelihood estimates based on the postulated and perturbed models, which are defined as  $\mathcal{P} = \{p(x; \theta) : \theta \in \Theta\}$  and,

$$\mathcal{P}_\omega = \{p(x; \theta, \omega) : \theta \in \Theta, \omega \in \Omega\}, \tag{6}$$

respectively, with  $\omega$  being a  $q$ -dimensional perturbation vector that is restricted to some open subset  $\Omega \subset \mathbb{R}^q$ . In addition, it is assumed that there is a null perturbation,  $\omega_0$ , satisfying  $\mathcal{P}_{\omega_0} = \mathcal{P}$ .

Note that objective functions other than the likelihood displacement can be used to assess the local influence (see, for instance, [Wu and Luo, 1993](#); [Cadigan and Farrel, 2002](#)). Let  $f(\omega)$  be a measure of influence. Thus, the main aim of the local influence approach is to analyze the curvature of the curves passing through the influence surface  $\varphi(\omega) = (\omega^\top, f(\omega))^\top$  at the critical point  $\omega_0$ . The idea is to find the direction associated to the largest normal curvature. This direction may evidence those observations that have considerable influence on the objective function under small perturbations on the postulated model and/or the data.

Consider  $\omega = \omega_0 + \varepsilon \mathbf{h}$ , where  $\mathbf{h}$  is a unitary direction ( $\|\mathbf{h}\| = 1$ ) and  $\varepsilon \in \mathbb{R}$ . We know from [Cook \(1986\)](#) that when the influence function  $f(\omega) = \text{LD}(\omega)$  is used, its local behavior around  $\varepsilon = 0$  for a direction  $\mathbf{h}$  can be characterized by the normal curvature  $C_h = \mathbf{h}^\top \ddot{\mathbf{F}} \mathbf{h}$ , where  $\ddot{\mathbf{F}} = \partial^2 \ell(\hat{\boldsymbol{\theta}}(\omega)) / \partial \omega \partial \omega^\top |_{\omega=\omega_0}$ . Moreover, [Cook \(1986\)](#) shows that  $\ddot{\mathbf{F}} = 2\boldsymbol{\Delta}^\top (-\ddot{\mathbf{L}})^{-1} \boldsymbol{\Delta}$  with

$$\ddot{\mathbf{L}} = \frac{\partial^2 \ell(\boldsymbol{\theta})}{\partial \boldsymbol{\theta} \partial \boldsymbol{\theta}^\top}, \quad \text{and} \quad \boldsymbol{\Delta} = \frac{\partial^2 \ell(\boldsymbol{\theta}|\omega)}{\partial \boldsymbol{\theta} \partial \omega^\top},$$

which must be evaluated at  $\boldsymbol{\theta} = \hat{\boldsymbol{\theta}}$  and  $\omega = \omega_0$ , and  $\ell(\boldsymbol{\theta})$  and  $\ell(\boldsymbol{\theta}|\omega)$  denote the log-likelihood functions arising from the postulated and perturbed models, respectively. The direction of maximum curvature  $\mathbf{h}_{\max}$  is determined by the eigenvector associated with the largest eigenvalue of the matrix  $\ddot{\mathbf{F}}$ . Such direction is used to identify which observations are locally influential. It is well known that  $C_h$  is not invariant under uniform changes in scale (see, for instance, [Fung and Kwan, 1997](#)). Thus, [Poon and Poon \(1999\)](#) proposed the conformal normal curvature, which is a scale-invariant influence measure and is given by  $B_h = \mathbf{h}^\top \ddot{\mathbf{F}} \mathbf{h} / \|\ddot{\mathbf{F}}\|_M$ , where  $\|\cdot\|_M$  denotes some matrix norm such as  $\|\ddot{\mathbf{F}}\|_M = (\text{tr}(\ddot{\mathbf{F}}^\top \ddot{\mathbf{F}}))^{1/2}$ . An interesting property of the conformal curvature is that  $0 \leq |B_h| \leq 1$ .

For general objective functions, we have that ([Cook, 1986](#)) the normal curvature assumes the form

$$C_{f,h} = \frac{\mathbf{h}^\top \mathbf{H}_f \mathbf{h}}{(1 + \nabla_f^\top \nabla_f) \mathbf{h}^\top (\mathbf{I} + \nabla_f \nabla_f^\top) \mathbf{h}}, \quad (7)$$

where  $\nabla_f = \partial f(\omega) / \partial \omega |_{\omega=\omega_0}$  and  $\mathbf{H}_f = \partial^2 f(\omega) / \partial \omega \partial \omega^\top |_{\omega=\omega_0}$ , whereas the conformal normal curvature in the direction  $\mathbf{h}$  evaluated at  $\omega_0$  ([Poon and Poon, 1999](#)) is given by

$$B_{f,h} = \frac{\mathbf{h}^\top \mathbf{H}_f \mathbf{h}}{\|\mathbf{H}_f\|_M \mathbf{h}^\top (\mathbf{I} + \nabla_f \nabla_f^\top) \mathbf{h}}. \quad (8)$$

According to matrix theory, the local maximum curvature and the corresponding directions are associated with the generalized eigenvalue-eigenvector solution of the equation  $|\mathbf{H}_f - \lambda \mathbf{D}_f| = 0$ , where  $\mathbf{D}_f$  is defined as  $(1 + \nabla_f^\top \nabla_f)(\mathbf{I} + \nabla_f \nabla_f^\top)$  or  $\|\mathbf{H}_f\|_M (\mathbf{I} + \nabla_f \nabla_f^\top)$  for the normal or conformal curvature, respectively.

The first-order approach for local influence (see for instance [Cadigan and Farrel, 2002](#)) is measured using the directional derivative of  $f(\omega)$ , which is given by

$$S_{f,h} = \left. \frac{\partial f(\omega)}{\partial \varepsilon} \right|_{\varepsilon=0} = \mathbf{h}^\top \nabla_f, \quad (9)$$

where  $\nabla_f = \partial f(\omega) / \partial \omega |_{\omega=\omega_0}$ . [Cadigan and Farrel \(2002\)](#) obtained a computationally simple formula for  $\nabla_f$ , which assumes the following form:

$$\nabla_f = -\boldsymbol{\Delta}^\top \ddot{\mathbf{L}}^{-1} \left. \frac{\partial f(\boldsymbol{\theta})}{\partial \boldsymbol{\theta}} \right|_{\boldsymbol{\theta}=\hat{\boldsymbol{\theta}}}.$$

In the case that  $\nabla_f \neq \mathbf{0}$ , the direction of the maximum local slope is  $\mathbf{h}_{\max} = \nabla_f / \|\nabla_f\|$ . Note that the first-order local influence may be unable to detect some significant directions with large curvature; (see

Wu and Luo, 1993; Cadigan and Farrel, 2002). It is straightforward to note that

$$\frac{\partial S_{f,h}}{\partial \varepsilon} \Big|_{\varepsilon=0} = \frac{\partial^2 f(\boldsymbol{\omega})}{\partial \varepsilon^2} \Big|_{\varepsilon=0} = \mathbf{h}^\top \left( \frac{\partial^2 f(\boldsymbol{\omega})}{\partial \boldsymbol{\omega} \partial \boldsymbol{\omega}^\top} \Big|_{\boldsymbol{\omega}=\boldsymbol{\omega}_0} \right) \mathbf{h} = \mathbf{h}^\top \mathbf{H}_f \mathbf{h}. \tag{10}$$

The perturbed model (6) can be regarded as an  $n$ -dimensional manifold with  $\boldsymbol{\omega}$  as a coordinate system. To construct influence measures of the first and second order, Zhu et al. (2007) introduced the metric tensor matrix  $\mathbf{G}(\boldsymbol{\omega})$  defined as the Fisher information matrix with respect to  $\boldsymbol{\omega}$ , with elements given by

$$g_{ij}(\boldsymbol{\omega}) = E_{\boldsymbol{\omega}} \left\{ \frac{\partial \ell(\boldsymbol{\theta}|\boldsymbol{\omega})}{\partial \omega_i} \frac{\partial \ell(\boldsymbol{\theta}|\boldsymbol{\omega})}{\partial \omega_j} \right\}, \quad \text{for } i, j = 1, \dots, n, \tag{11}$$

where  $E_{\boldsymbol{\omega}}(\cdot)$  indicates that the expectation is taken with respect to the density function  $p(\mathbf{x}; \boldsymbol{\theta}, \boldsymbol{\omega})$ . Thus, the first-order influence measure (FI) in the direction  $\mathbf{h}$  is given by

$$FI_{f,h} = \frac{\mathbf{h}^\top \nabla_f \nabla_f^\top \mathbf{h}}{\mathbf{h}^\top \mathbf{G}(\boldsymbol{\omega}_0) \mathbf{h}}, \tag{12}$$

where  $\mathbf{G}(\boldsymbol{\omega}_0)$  is the metric tensor matrix evaluated at  $\boldsymbol{\omega}_0$ . The second-order influence measure (SI) in the direction  $\mathbf{h}$  is given by

$$SI_{f,h} = \frac{\mathbf{h}^\top \tilde{\mathbf{H}}_f \mathbf{h}}{\mathbf{h}^\top \mathbf{G}(\boldsymbol{\omega}_0) \mathbf{h}}, \tag{13}$$

with  $\tilde{\mathbf{H}}_f$  being the covariant Hessian matrix at  $\boldsymbol{\omega}_0$ , where the  $(i, j)$ th element is given by

$$(\tilde{\mathbf{H}}_f)_{ij} = \frac{\partial}{\partial \omega_i} \left( \frac{\partial f(\boldsymbol{\omega})}{\partial \omega_j} \right) \Big|_{\boldsymbol{\omega}=\boldsymbol{\omega}_0} - \sum_{s,r} g^{r,s}(\boldsymbol{\omega}) \Gamma_{ijs}^0(\boldsymbol{\omega}) \left( \frac{\partial f(\boldsymbol{\omega})}{\partial \omega_r} \right) \Big|_{\boldsymbol{\omega}=\boldsymbol{\omega}_0},$$

in which  $g^{r,s}(\boldsymbol{\omega})$  is the  $(r, s)$ th element of  $\mathbf{G}(\boldsymbol{\omega})^{-1}$  and

$$\Gamma_{ijs}^0(\boldsymbol{\omega}) = \frac{1}{2} \left\{ \frac{\partial}{\partial \omega_i} g(\boldsymbol{\omega})_{js} + \frac{\partial}{\partial \omega_j} g_{is}(\boldsymbol{\omega}) - \frac{\partial}{\partial \omega_s} g_{ij}(\boldsymbol{\omega}) \right\},$$

denotes the Christoffel symbol for the Lévi-Civita connection.

Zhu et al. (2007) proposed to investigate how the introduced perturbation  $\boldsymbol{\omega}$  affects the postulated model  $\mathcal{P}$ . Consider the case-weight perturbation scheme with perturbed log-likelihood function given by

$$\ell(\boldsymbol{\theta}|\boldsymbol{\omega}) = \sum_{i=1}^n \omega_i \ell_i(\boldsymbol{\theta}), \quad \text{with } \boldsymbol{\omega} = (\omega_1, \dots, \omega_n)^\top \in \mathbb{R}^n, \tag{14}$$

and  $\ell_i(\boldsymbol{\theta})$  being defined in Equation (4). Thus, the density of the perturbed model yielding the log-likelihood function in (14) takes the form (see Equation (17) of Zhu et al., 2007)

$$p(\mathbf{x}; \boldsymbol{\theta}, \boldsymbol{\omega}) = \prod_{i=1}^n \exp(\omega_i \ell_i(\boldsymbol{\theta})) / c_i(\omega_i; \boldsymbol{\theta}), \quad c_i(\omega_i, \boldsymbol{\theta}) = \int_{\mathbb{R}^d} \exp(\omega_i \ell_i(\boldsymbol{\omega})) \, d\mathbf{x}_i.$$

Next, we present necessary formulas required to obtain normal and conformal curvatures and first- and second-order influence measures using Equations (7), (8) and (12), (13), respectively. Moreover, for the case-weight perturbation defined in (14), we have that the elements of the metric tensor matrix are given by  $g_{ij}(\boldsymbol{\omega}) = \delta_{ij} \omega_i^2$ , where  $\delta_{ij}$  is the Kronecker delta. Then,  $\mathbf{G}(\boldsymbol{\omega}_0) = \mathbf{I}_n$ , and we verify that the perturbation scheme induced by the model  $\mathcal{P}_\omega$  in (18) is appropriate (Zhu et al., 2007).

### 3.2 Influence measures for the concordance correlation coefficient and the probability of agreement

Following Wu and Luo (1993), we consider  $\hat{\rho}_c(\boldsymbol{\omega})$  and  $\hat{\psi}_c(\boldsymbol{\omega})$  as objective functions, defined respectively by

$$\hat{\rho}_c(\boldsymbol{\omega}) = \frac{2\hat{\sigma}_{12}(\boldsymbol{\omega})}{\hat{\sigma}_{11}(\boldsymbol{\omega}) + \hat{\sigma}_{22}(\boldsymbol{\omega}) + (\hat{\mu}_1(\boldsymbol{\omega}) - \hat{\mu}_2(\boldsymbol{\omega}))^2}, \quad (15)$$

and

$$\hat{\psi}_c(\boldsymbol{\omega}) = \Phi\left(\frac{c - \hat{\mu}_D(\boldsymbol{\omega})}{\hat{\sigma}_D(\boldsymbol{\omega})}\right) - \Phi\left(-\frac{c - \hat{\mu}_D(\boldsymbol{\omega})}{\hat{\sigma}_D(\boldsymbol{\omega})}\right), \quad (16)$$

where  $\hat{\mu}_D(\boldsymbol{\omega}) = \hat{\mu}_1(\boldsymbol{\omega}) - \hat{\mu}_2(\boldsymbol{\omega})$ ,  $\hat{\sigma}_D^2(\boldsymbol{\omega}) = \hat{\sigma}_{11}(\boldsymbol{\omega}) + \hat{\sigma}_{22}(\boldsymbol{\omega}) - 2\hat{\sigma}_{12}(\boldsymbol{\omega})$ , and

$$\hat{\mu}_j(\boldsymbol{\omega}) = \frac{1}{\sum_{i=1}^n \omega_i} \sum_{i=1}^n \omega_i X_{ij}, \quad \hat{\sigma}_{jk}(\boldsymbol{\omega}) = \frac{1}{\sum_{i=1}^n \omega_i} \sum_{i=1}^n \omega_i (X_{ij} - \hat{\mu}_j(\boldsymbol{\omega}))(X_{ik} - \hat{\mu}_k(\boldsymbol{\omega})), \quad (17)$$

for  $j, k = 1, 2$ , and  $\boldsymbol{\omega} = (\omega_1, \dots, \omega_n)^\top$ . Thus,  $\varphi(\boldsymbol{\omega}) = (\boldsymbol{\omega}^\top, \hat{\rho}_c(\boldsymbol{\omega}))^\top$  and  $\varphi(\boldsymbol{\omega}) = (\boldsymbol{\omega}^\top, \hat{\psi}_c(\boldsymbol{\omega}))^\top$  are called the CCC and the probability of agreement surfaces, respectively.

Under the Gaussian assumption, it is straightforward to note that

$$c_i(\omega_i, \boldsymbol{\theta}) = \int_{\mathbb{R}^d} |2\pi\Sigma|^{-\omega_i/2} \exp\left\{-\frac{1}{2}\omega_i(\mathbf{x}_i - \boldsymbol{\mu})^\top \Sigma^{-1}(\mathbf{x}_i - \boldsymbol{\mu})\right\} d\mathbf{x}_i = \frac{|2\pi\Sigma|^{-\omega_i/2}}{|2\pi\omega_i^{-1}\Sigma|^{-1/2}},$$

leading to the density of the perturbed model, which is given by

$$p(\mathbf{x}; \boldsymbol{\theta}, \boldsymbol{\omega}) = \prod_{i=1}^n \left[ (2\pi)^{-d/2} |\omega_i^{-1}\Sigma|^{-1/2} \exp\left\{-\frac{1}{2}\omega_i(\mathbf{x}_i - \boldsymbol{\mu})^\top \Sigma^{-1}(\mathbf{x}_i - \boldsymbol{\mu})\right\} \right]. \quad (18)$$

Note that the vector of the null perturbation is given by  $\boldsymbol{\omega}_0 = \mathbf{1}_n$  in which case  $\mathcal{P}_{\boldsymbol{\omega}_0} = \mathcal{P}$  and  $\ell(\boldsymbol{\theta}|\boldsymbol{\omega}_0) = \ell(\boldsymbol{\theta})$ . As in Galea and Giménez (2016), the first- and second-order influence measures are reduced to

$$\text{FI}_{f,h} = \mathbf{h}^\top \nabla_f \nabla_f^\top \mathbf{h}, \quad \text{and} \quad \text{SI}_{f,h} = \mathbf{h}^\top \tilde{\mathbf{H}}_f \mathbf{h},$$

respectively, for each objective function, either  $\hat{\rho}_c(\boldsymbol{\omega})$  or  $\hat{\psi}_c(\boldsymbol{\omega})$ . The first-order derivative required in  $\text{FI}_{\hat{\rho}_c,h}$ , as well as  $C_{\hat{\rho}_c,h}$  and  $B_{\hat{\rho}_c,h}$ , assumes the form

$$\nabla_{\hat{\rho}_c} = \frac{\hat{\rho}_c}{n\hat{\sigma}_{12}} (\mathbf{Z}_1 \odot \mathbf{Z}_2 - \hat{\sigma}_{12}\mathbf{1}) - \frac{\hat{\rho}_c^2}{2n\hat{\sigma}_{12}} \mathbf{Z}_*, \quad (19)$$

where  $\mathbf{Z}_j = (Z_{1j}, \dots, Z_{nj})^\top$  with  $Z_{ij} = X_{ij} - \hat{\mu}_j$ , for  $i = 1, \dots, n$ ;  $j = 1, 2$  and  $\odot$  represents the Hadamard product. Moreover,  $\tilde{\mathbf{H}}_{\hat{\rho}_c} = \mathbf{H}_{\hat{\rho}_c} + \text{diag}(\nabla_{\hat{\rho}_c})$ , with

$$\mathbf{H}_{\hat{\rho}_c} = \boldsymbol{\Gamma}_1 - (\boldsymbol{\Gamma}_2 + \boldsymbol{\Gamma}_3). \quad (20)$$

The calculations of (19) and (20) are given in the Appendix B. Whereas  $\nabla_{\hat{\psi}_c} = \partial \hat{\psi}_c(\boldsymbol{\omega}) / \partial \boldsymbol{\omega}|_{\boldsymbol{\omega}=\boldsymbol{\omega}_0}$  assumes the form

$$\nabla_{\hat{\psi}_c} = -\frac{2}{\hat{\sigma}_D^2} \phi\left(\frac{c - \hat{\mu}_D}{\hat{\sigma}_D}\right) \mathbf{s}, \quad (21)$$



with

$$\mathbf{s} = \hat{\sigma}_D(\mathbf{Z}_1 - \mathbf{Z}_2) + \frac{1}{2} \left( \frac{c - \hat{\mu}_D}{\hat{\sigma}_D} \right) \left\{ \frac{n-2}{n} (\mathbf{Z}_1 - \mathbf{Z}_2) \odot (\mathbf{Z}_1 - \mathbf{Z}_2) - \hat{\sigma}_D^2 \mathbf{1} \right\}. \quad (22)$$

In addition,  $\mathbf{H}_{\hat{\psi}_c} = \partial^2 \hat{\psi}_c(\boldsymbol{\omega}) / \partial \boldsymbol{\omega} \partial \boldsymbol{\omega}^\top$  can be written as,

$$\mathbf{H}_{\hat{\psi}_c} = 2\phi \left( \frac{c - \hat{\mu}_D}{\hat{\sigma}_D} \right) \left\{ \boldsymbol{\Delta}_1 - \frac{1}{\hat{\sigma}_D^2} (\boldsymbol{\Delta}_2 + \boldsymbol{\Delta}_3 + \boldsymbol{\Delta}_4) - \frac{1}{\hat{\sigma}_D^4} \mathbf{s} \mathbf{s}^\top \right\}. \quad (23)$$

Details on the derivation of (21) and (23) can be found in Appendix C.

To identify influential observations on  $\hat{\rho}_c(\boldsymbol{\omega})$  or  $\hat{\psi}_c(\boldsymbol{\omega})$ , we shall now inspect the unitary direction  $\mathbf{h}_{\max}$ , corresponding to the maximum absolute value of  $\text{FI}_{f,h}$  and  $\text{SI}_{f,h}$  (equivalently,  $C_{f,h}$  and  $B_{f,h}$ ) given by the largest absolute eigenvalue of  $\nabla_f \nabla_f^\top$  and  $\tilde{\mathbf{H}}_f$  (generalized eigenvalue of  $\mathbf{H}_f$  with respect to  $(1 + \|\nabla_f\|^2)(\mathbf{I} + \nabla_f \nabla_f^\top)$  and  $\|\mathbf{H}_f\|_M(\mathbf{I} + \nabla_f \nabla_f^\top)$ ) for each objective function  $\hat{\rho}_c(\boldsymbol{\omega})$  or  $\hat{\psi}_c(\boldsymbol{\omega})$ , respectively. High-order influential cases are the observations with strong influence compared with the average  $\bar{M}$  of the values  $M_j = |\mathbf{h}_{\max}|_j$  for all the cases.  $\bar{M} + 2 \text{sd}(M)$ , where  $\text{sd}(M)$  denotes the standard deviation of  $M_j, j = 1, \dots, n$  can be used as a benchmark to determine the significance of contributions for an individual case. We consider this benchmark in our empirical studies of Section 4.

### 4 Simulation study

In our experiment, 500 datasets with a sample size of  $n = 25, 50, 100$  and  $200$  from a normal distribution with mean vector  $\boldsymbol{\mu} = (0, 0)^\top$  and  $\boldsymbol{\phi} = (1, 0.95, 1)^\top$  were generated. To introduce an outlier, for each dataset, a single observation of the second variable  $x_2$  was changed to  $x_2 + \delta$ , where  $\delta = 0.5, 1.5, 2.0, 2.5, 3.0$  and  $3.5$ . Next, we find the unitary direction related to the maximum local slope, normal and conformal curvatures and first- and second-order influence measures for the objective functions  $\hat{\rho}_c(\boldsymbol{\omega})$  and  $\hat{\psi}_c(\boldsymbol{\omega})$ . Thus, the percentages of detecting the outlier are computed using the threshold mentioned above for different values of  $\delta$ .

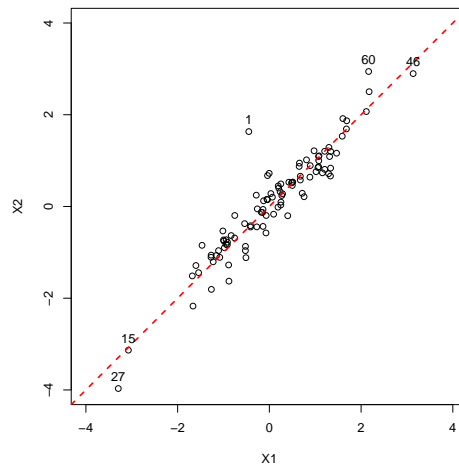


**Figure 4** Scatter plot of a typical dataset (with  $\delta = 2$ ) from the simulation experiment

Tables 3 and 4 present the detection percentage of the single outlier under the case-weight perturbation scheme. As expected, the outlier detection percentages improve as  $\delta$  increases. Our findings seem to suggest that, when the perturbed CCC is used as objective function, the second-order influence measures are more conservative in detecting a single outlier, whereas the FI influence measure and the local maximum slope were more efficient for the detection of this type of outlier for any value of  $\delta$  (compare with the simulation results presented by Galea and Giménez, 2016). Figures 5 and 6 present the influence graphs for a typical dataset considering  $\delta = 2$  (see Figure 4). This plot reveals that second-order procedures may be unable to identify the introduced outlier. We must highlight that using the FI and SI measures together achieve a lower detection percentage than using only FI or SI. Moreover, this difference seems more significant for moderate values of  $\delta$ . It is interesting to note that when the probability of agreement is perturbed (with  $c = 2$ ) allow us a better detection of extreme observations. In addition all the influence methods present a similar performance (see Table 4).

**Table 3** Outlier detection percentage using different influence measures:  $\hat{\rho}_c(\omega)$  as objective function

$n$	Influence measure	$\delta$						
		0.5	1.0	1.5	2.0	2.5	3.0	3.5
25	$C$	11.4	33.8	66.4	77.8	86.4	93.4	95.4
	$B$	11.4	33.8	66.4	77.8	86.4	93.4	95.4
	FI	28.4	74.4	96.0	99.0	99.8	100.0	100.0
	SI	11.4	33.8	66.4	77.8	86.4	93.4	95.4
	FI and SI	6.4	27.4	63.2	76.8	86.2	93.4	95.4
50	$C$	9.6	34.2	59.4	77.4	90.0	96.4	97.0
	$B$	9.6	34.2	59.4	77.4	90.0	96.4	97.0
	FI	26.0	76.0	96.4	100.0	100.0	100.0	100.0
	SI	9.6	34.2	59.4	77.4	90.0	96.4	97.0
	FI and SI	5.6	28.4	58.0	77.4	90.0	96.4	97.0
100	$C$	11.8	30.8	53.8	74.8	92.4	98.4	98.0
	$B$	11.8	30.8	53.8	74.8	92.4	98.4	98.0
	FI	27.0	77.2	97.2	100.0	100.0	100.0	100.0
	SI	11.8	30.8	53.8	74.8	92.4	98.4	98.0
	FI and SI	8.8	26.8	52.8	74.8	92.4	98.4	98.0
200	$C$	16.0	42.8	58.2	68.0	89.6	98.2	99.0
	$B$	16.0	42.8	58.2	68.0	89.6	98.2	99.0
	FI	26.4	79.2	97.2	100.0	100.0	100.0	100.0
	SI	16.0	42.8	58.2	68.0	89.6	98.2	99.0
	FI and SI	9.6	36.6	57.0	68.0	89.6	98.2	99.0

We further investigate the empirical performance of the proposal influence measures, based on a simulation experiment with two added outliers (observations 1 and 10). We must stress that the behavior is quite similar for the case of two outliers although as expected the detection rates increase at a slower rate (in terms of  $\delta$  increment) than the case of a single outlier. These simulation results are deferred to the Supplementary Material.

## 5 Real-world application: Transient sleep disorder

Here, we consider the clinical trial about insomnia problems described in Section 2.1. This dataset was previously analyzed by Feng et al. (2015) using a robust approach within a Bayesian framework. Figure 1 reveals that observations 1, 30 and 79 are outside the limits of agreement and therefore can be identified

**Table 4** Outlier detection percentage using different influence measures:  $\hat{\psi}_c(\omega)$  as objective function

$n$	Influence measure	$\delta$						
		0.5	1.0	1.5	2.0	2.5	3.0	3.5
25	$C$	24.6	77.6	98.2	100.0	100.0	100.0	100.0
	$B$	24.6	77.6	98.2	100.0	100.0	100.0	100.0
	FI	26.4	81.4	98.6	100.0	100.0	100.0	100.0
	SI	24.6	77.6	98.2	100.0	100.0	100.0	100.0
	FI and SI	24.6	77.4	98.2	100.0	100.0	100.0	100.0
50	$C$	23.4	74.0	97.8	100.0	100.0	100.0	100.0
	$B$	23.4	74.0	97.8	100.0	100.0	100.0	100.0
	FI	27.0	81.4	98.2	100.0	100.0	100.0	100.0
	SI	23.4	74.0	97.8	100.0	100.0	100.0	100.0
	FI and SI	23.4	74.0	97.6	100.0	100.0	100.0	100.0
100	$C$	17.2	58.8	94.6	99.8	100.0	100.0	100.0
	$B$	17.2	58.8	94.6	99.8	100.0	100.0	100.0
	FI	26.8	82.2	98.4	100.0	100.0	100.0	100.0
	SI	17.2	58.8	94.6	99.8	100.0	100.0	100.0
	FI and SI	16.8	58.2	94.6	99.8	100.0	100.0	100.0
200	$C$	16.8	59.4	89.2	98.8	100.0	100.0	100.0
	$B$	16.8	59.4	89.2	98.8	100.0	100.0	100.0
	FI	27.4	83.6	98.8	100.0	100.0	100.0	100.0
	SI	16.8	59.4	89.2	98.8	100.0	100.0	100.0
	FI and SI	15.8	57.4	89.0	98.8	100.0	100.0	100.0

as potential outliers. It is interesting to note the role of these observations when they are removed from the data set; observations 1, 30 and 79 do not have an impact on the estimation of the mean vector. This analysis reveals the high sensitivity of the variance and CCC estimates, with percent changes of -66% and 28%, for  $\det(\hat{\Sigma})$  and  $\hat{\rho}_c$ , respectively. Whereas the PA appears to be quite less sensitive to the removal of these extreme observations (see Tables 5 and 6).

**Table 5** Percentage changes of the ML estimates for the fitted model.

Estimate	with all observations	obs. 1,30,79 removed	change (%)
$\hat{\mu}_1$	2.554	2.526	-1.090
$\hat{\mu}_2$	2.309	2.313	0.190
$\det(\hat{\Sigma})$	0.460	0.156	-66.171

To detect influential observations, we employed the diagnostic measures described in Section 3.2, which have been implemented in an R code available at github (<https://github.com/faosorios/CCC/>). The analysis of the first two generalized eigenvectors of the  $C_{\hat{\rho}_c, h}$  curvature (see Figures 7a and b) indicated that observations 30 and 79 were influential, with slightly less influence for observation 1. Moreover, Figure 7b shows that observation 79 is highly influential along the direction  $|h_{2nd}|$  (the index plot of the  $B_{\hat{\rho}_c, h}$  curvature is not presented here because it is very similar to the one displayed in Figure 7a).  $FI_{\hat{\rho}_c, h}$  and  $SI_{\hat{\rho}_c, h}$  also allow one to detect cases 1, 30 and 79 as influential on the CCC estimate. The time savings in terms of the computational burden of the first-order approach should be stressed. Moreover, for this approach,  $h_{max}$  was explicitly obtained. The local influence analysis applied on the PA function allows

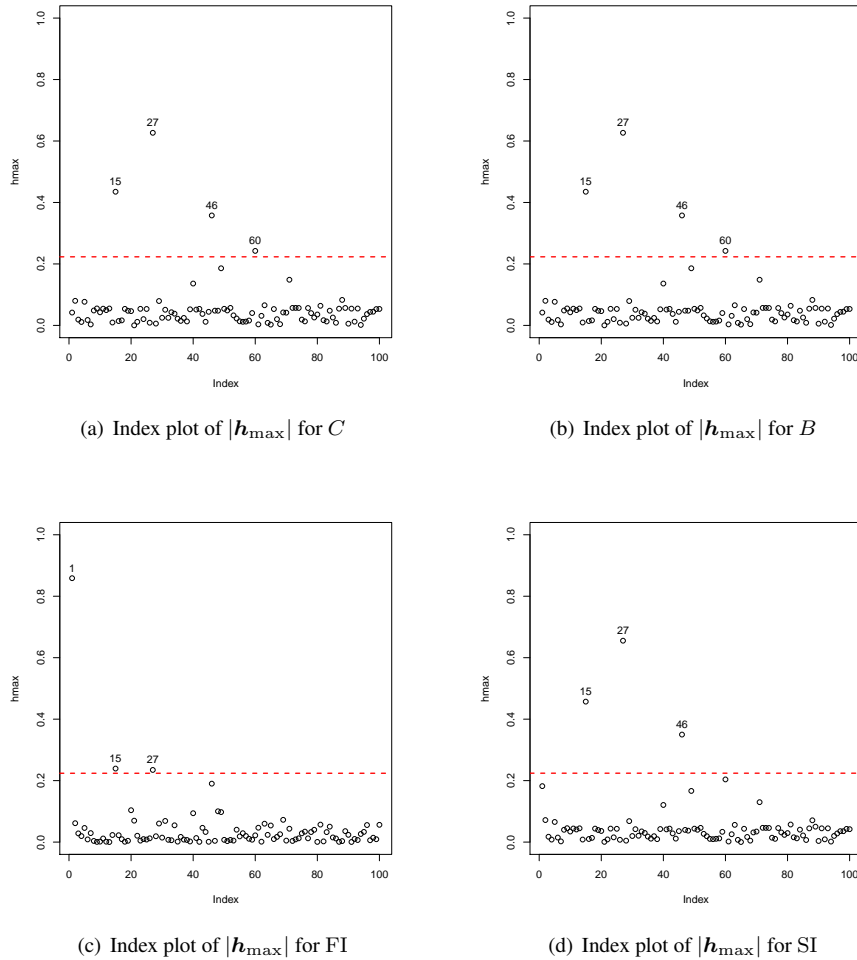


**Figure 5** Index plot of  $|h_{\max}|$  under case-weight scheme for (a) normal curvature, (b) conformal curvature, (c) first- and (d) second-order influence measures for the simulated data:  $\hat{\rho}_c(\omega)$  as objective function.

to note that, although all the procedures are able to detect the observations 1, 30 and 79. The first-order influence presents a better power of detection.

With the objective of investigating the sensitivity of the CCC estimate, a confirmatory study was conducted, therein consisting of removing the following sets of observations  $I_1 = \{1, 30, 79\}$  and  $I_2 = \{1, 30, 35, 79\}$  and computing the percentage change in the estimation of CCC. We must emphasize that the percentage change (28%) when subset  $I_1$  is removed (see Table 6) increases by only 2% when  $I_2$  is removed from the dataset. These results confirm the analyses of Feng et al. (2015) and reveal the extreme sensitivity of the CCC estimate under the normal assumption. Furthermore, we examine the sensitivity of the CCC estimate by exploring the effect of subset  $I_1$  on the standard error and confidence intervals considering several methods (Table 7), specifically, the normal approximation,  $Z$ -Fisher transformation and bootstrap. Again, we note the strong effect of dropping subset  $I_1$ , confirming that observations 1, 30 and 72 are influential data.

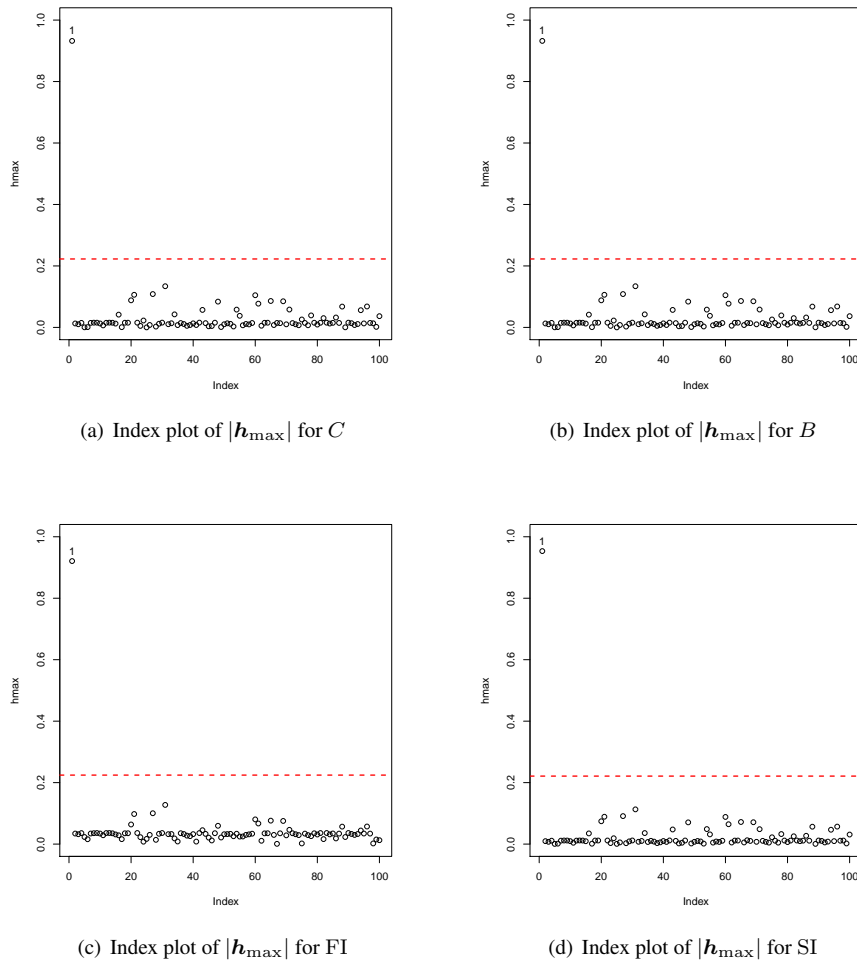


**Figure 6** Index plot of  $|h_{\max}|$  under case-weight scheme for (a) normal curvature, (b) conformal curvature, (c) first- and (d) second-order influence measures for the simulated data:  $\hat{\psi}_c(\omega)$  as objective function.

## 6 Concluding remarks

Evaluating the sensitivity of the ML estimates for the CCC and the probability of agreement against atypical observations is an important step in the analysis of agreement. These influential data may distort the estimation of the coefficient and lead to incorrect decisions, like replacing one measurement method with another when their degree of agreement is not really true.

The goal of our work was to propose diagnostic measures to detect data that can exert a strong influence on the estimates of the CCC and the probability of agreement. It was shown that the case-weight perturbation scheme is appropriate in the sense defined by [Zhu et al. \(2007\)](#). Closed expressions have been provided for the matrices required to evaluate the influence measures. A computational implementation of such diagnostic techniques has been made publicly available. The empirical results seem to suggest that for the problem under study, first-order influence measures are efficient for the identification of influential observations, whereas second-order measures were not very powerful. The results are confirmed by a

**Table 6** Percentage changes for  $\hat{\rho}_c$  and  $\hat{\psi}_c$  estimates, log-likelihood and Akaike information criterion

Observations removed	$\hat{\rho}_c$	change (%)	$\hat{\psi}_c$	change (%)	log-likelihood	AIC
—	0.674	—	0.975	—	-200.890	411.780
1	0.715	6	0.986	1	-192.990	395.979
30	0.749	11	0.992	2	-186.448	382.897
79	0.724	7	0.990	1	-185.907	381.815
1, 30	0.795	18	0.997	2	-175.741	361.482
1, 79	0.770	14	0.996	2	-175.982	361.963
30, 79	0.808	20	0.999	2	-166.688	343.376
1, 30, 79	0.860	28	1.000	3	-150.728	311.456

**Table 7** CCC estimates (standard errors in parenthesis) and asymptotic confidence interval considering normal approximation,  $Z$ -Fisher transformation and Bootstrap. Clinical trial data set.

Method	All observations		Obs. 1, 30 and 79 removed	
	Estimate	Conf. Interval	Estimate	Conf. Interval
Normal	0.674 (0.056)	(0.564, 0.785)	0.860 (0.023)	(0.805, 0.915)
$Z$ -Fisher	0.674 (0.103)	(0.549, 0.770)	0.860 (0.107)	(0.795, 0.906)
Bootstrap	0.675 (0.104)	(0.472, 0.878)	0.861 (0.041)	(0.782, 0.944)

simulation study. Although there is not much literature on the assessment of local influence for objective functions with non-zero first derivatives at the critical point, we must stress that the results allow us to recommend the identification of influential observations through the combined use of first- and second-order measures. In addition, our findings are in agreement with the results reported by Feng et al. (2015), who used an approach for the robust estimation of the CCC suitable for the comparison of various measurement instruments.

Further work in this area includes extending the estimation and diagnostics for the CCC and the probability of agreement considering a multivariate  $t$ -distribution. Although such models can accommodate extreme observations, they can still be affected by outlying observations. This topic is being developed by the authors and will be the subject of a forthcoming paper.


**Acknowledgements** The authors are grateful to Dai Feng and Vladimir Svetnik from Merck & Co. Inc. for providing the data about transient sleep disorder. This work was supported by Comisión Nacional de Investigación Científica y Tecnológica, FONDECYT grants 1140580 and 1150325. The authors acknowledge the suggestions from two anonymous referees and an associate editor which helped to improve the manuscript.


### Conflict of Interest

*The authors have declared no conflict of interest.*

### ORCID

Carla Leal  <http://orcid.org/0000-0003-1739-3456>

Manuel Galea  <http://orcid.org/0000-0001-9819-5843>

Felipe Osorio  <http://orcid.org/0000-0002-4675-5201>

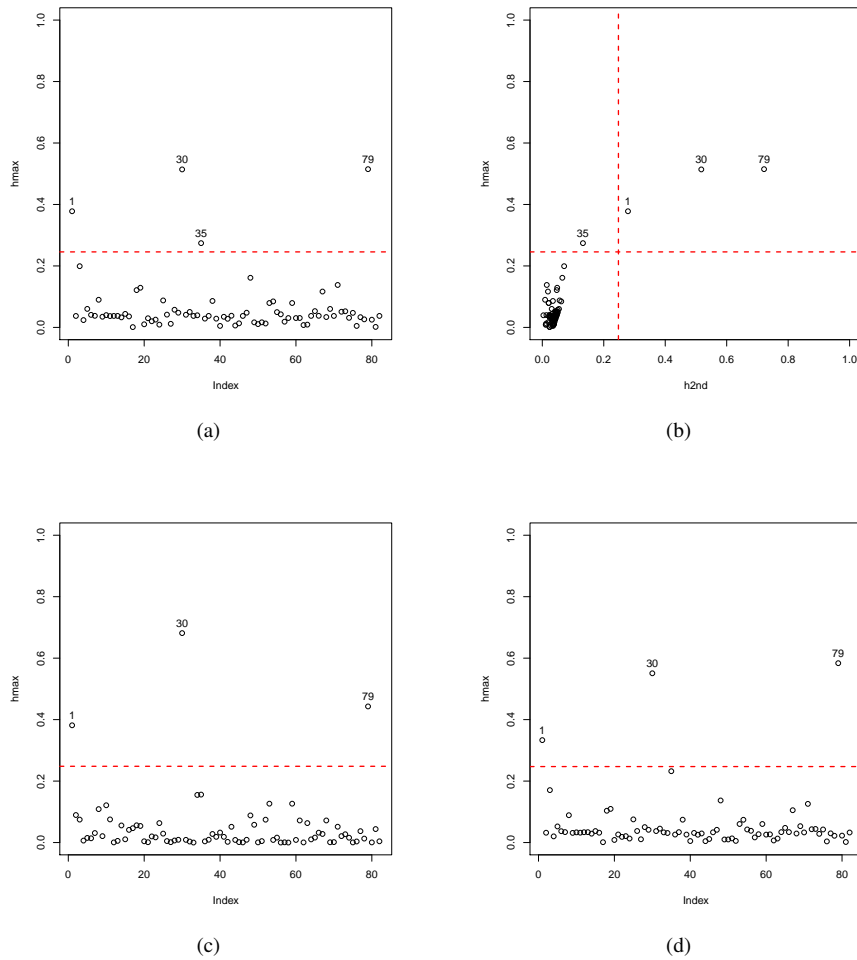


**Figure 7** Index plot of  $|h_{\max}|$  for (a) normal curvature, (b)  $|h_{\max}|$  against  $|h_{2nd}|$  for normal curvature, index plot of  $|h_{\max}|$  for (c) FI and (d) SI influence measures:  $\hat{\rho}_c(\omega)$  as objective function.

**Appendix A: Asymptotic normality of the ML estimator for the probability of agreement**

Let  $\hat{\theta} = (\hat{\mu}^\top, \text{vech}^\top \hat{\Sigma})^\top$  the ML estimator of  $\mu$  and  $\phi$  under the normality assumption. We know that

$$\sqrt{n}(\hat{\theta} - \theta) \xrightarrow{D} \mathcal{N}_{d_*}(\mathbf{0}, \mathbf{J}(\theta)),$$

with  $d_* = d(d + 3)/2$  ( $d = 2$ ), and

$$\mathbf{J}(\theta) = \begin{pmatrix} \Sigma & \mathbf{0} \\ \mathbf{0} & 2D_d^\top (I_{d^2} + K_d)(\Sigma \otimes \Sigma)D_d \end{pmatrix},$$

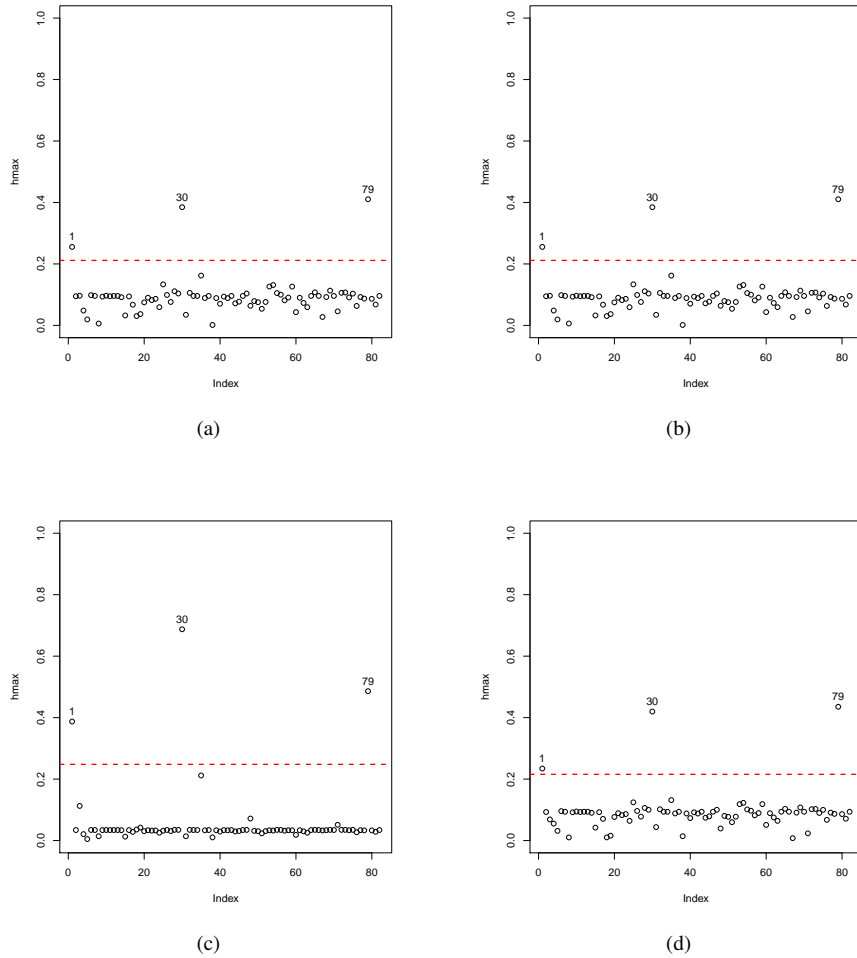


**Figure 8** Index plot of  $|h_{\max}|$  for (a) normal curvature, (b)  $|h_{\max}|$  against  $|h_{2\text{nd}}|$  for normal curvature, index plot of  $|h_{\max}|$  for (c) FI and (d) SI influence measures:  $\hat{\psi}_c(\omega)$  as objective function.

where  $D_d \in \mathbb{R}^{d^2 \times d(d+1)/2}$  and  $K_d \in \mathbb{R}^{d^2 \times d^2}$  denote the duplication and commutation matrices, respectively (see Magnus and Neudecker, 2007, Sec. 3.7 and 3.8). Using the Delta method, follows that

$$\sqrt{n}(\hat{\psi}_c - \psi_c) \xrightarrow{D} \mathcal{N}_1\left(0, \left(\frac{\partial \psi_c}{\partial \theta}\right)^\top \mathbf{J}(\theta) \frac{\partial \psi_c}{\partial \theta}\right),$$

where  $\partial \psi_c / \partial \theta$  and  $\mathbf{J}(\theta)$  must be evaluated at  $\theta = \hat{\theta}$ . It is straightforward to note that

$$\frac{\partial \psi_c}{\partial \theta} = \frac{1}{\sigma_D} \phi\left(\frac{c - \mu_D}{\sigma_D}\right) \left(-2, 2, -\frac{(c - \mu_D)/\sigma_D}{\sigma_D}, \frac{2(c - \mu_D)/\sigma_D}{\sigma_D}, -\frac{(c - \mu_D)/\sigma_D}{\sigma_D}\right)^\top.$$



Thus, the asymptotic variance of  $\widehat{\psi}_c$  assumes the form

$$\begin{aligned} \text{var}(\widehat{\psi}_c) &= \frac{1}{n} \left( \frac{\partial \psi_c}{\partial \boldsymbol{\theta}} \right)^\top \mathbf{J}(\boldsymbol{\theta}) \frac{\partial \psi_c}{\partial \boldsymbol{\theta}} \\ &= \frac{2}{n\sigma_D^2} \phi^2 \left( \frac{c - \mu_D}{\sigma_D} \right) \left[ \sigma_D^2 + \frac{1}{\sigma_D^2} \left( \frac{c - \mu_D}{\sigma_D} \right)^2 \{ \sigma_{11}^2 + \sigma_{22}^2 + 2\sigma_{12}^2 + 8(\sigma_{11} - \sigma_{12})(\sigma_{22} - \sigma_{12}) \} \right], \end{aligned}$$

which must be evaluated at  $\boldsymbol{\theta} = \widehat{\boldsymbol{\theta}}$ .

### Appendix B: Proof of Equations (19) and (20)

The perturbed estimator of the concordance correlation coefficient is given by

$$\widehat{\rho}_c(\boldsymbol{\omega}) = \frac{2\widehat{\sigma}_{12}(\boldsymbol{\omega})}{\widehat{\sigma}_{11}(\boldsymbol{\omega}) + \widehat{\sigma}_{22}(\boldsymbol{\omega}) + (\widehat{\mu}_1(\boldsymbol{\omega}) - \widehat{\mu}_2(\boldsymbol{\omega}))^2},$$

where  $\boldsymbol{\omega} = \boldsymbol{\omega}_0 + \varepsilon \mathbf{h}$  and the perturbed ML estimator  $\widehat{\boldsymbol{\theta}}(\boldsymbol{\omega}) = (\widehat{\mu}_1(\boldsymbol{\omega}), \widehat{\mu}_2(\boldsymbol{\omega}), \widehat{\sigma}_{11}(\boldsymbol{\omega}), \widehat{\sigma}_{12}(\boldsymbol{\omega}), \widehat{\sigma}_{22}(\boldsymbol{\omega}))^\top$  is defined in Equation (17). Next, we find the first and second derivative of  $\widehat{\rho}_c(\boldsymbol{\omega})$  under the case-weight perturbation scheme introduced in (14).

Let

$$\beta_j(\boldsymbol{\omega}) = \frac{d\widehat{\mu}_j(\boldsymbol{\omega})}{d\varepsilon}, \quad \alpha_{jk}(\boldsymbol{\omega}) = \frac{d\widehat{\sigma}_{jk}(\boldsymbol{\omega})}{d\varepsilon},$$

be the first derivative of the perturbed ML estimator of  $\mu_j(\boldsymbol{\omega})$  and  $\sigma_{jk}(\boldsymbol{\omega})$  with respect to  $\varepsilon$ , for  $j, k = 1, 2$ . Thus, we obtain

$$\begin{aligned} \beta_1(\boldsymbol{\omega})|_{\varepsilon=0} &= \mathbf{h}^\top \frac{\mathbf{Z}_1}{n}, & \beta_2(\boldsymbol{\omega})|_{\varepsilon=0} &= \mathbf{h}^\top \frac{\mathbf{Z}_2}{n} \\ \alpha_{11}(\boldsymbol{\omega})|_{\varepsilon=0} &= \mathbf{h}^\top \frac{\mathbf{Z}_1 \odot \mathbf{Z}_1 - \widehat{\sigma}_{11} \mathbf{1}_n}{n}, & \alpha_{12}(\boldsymbol{\omega})|_{\varepsilon=0} &= \mathbf{h}^\top \frac{\mathbf{Z}_1 \odot \mathbf{Z}_2 - \widehat{\sigma}_{12} \mathbf{1}_n}{n}, \\ \alpha_{22}(\boldsymbol{\omega})|_{\varepsilon=0} &= \mathbf{h}^\top \frac{\mathbf{Z}_2 \odot \mathbf{Z}_2 - \widehat{\sigma}_{22} \mathbf{1}_n}{n}, \end{aligned}$$

where  $\odot$  is the Hadamard product,  $\mathbf{Z}_1 = (Z_{11}, \dots, Z_{n1})^\top$ ,  $\mathbf{Z}_2 = (Z_{12}, \dots, Z_{n2})^\top$  and  $Z_{ij} = X_{ij} - \widehat{\mu}_j$  for  $i = 1, \dots, n$  and  $j = 1, 2$ .

This leads to the first derivative of the perturbed ML estimator of the CCC, which is given by

$$\begin{aligned} \frac{d\widehat{\rho}_c(\boldsymbol{\omega})}{d\varepsilon} \Big|_{\varepsilon=0} &= \frac{2(d\widehat{\sigma}_{12}(\boldsymbol{\omega})/d\varepsilon)}{\widehat{\sigma}_{11}(\boldsymbol{\omega}) + \widehat{\sigma}_{22}(\boldsymbol{\omega}) + (\widehat{\mu}_1(\boldsymbol{\omega}) - \widehat{\mu}_2(\boldsymbol{\omega}))^2} \Big|_{\varepsilon=0} \\ &\quad - \frac{2\widehat{\sigma}_{12}(\boldsymbol{\omega}) d(\widehat{\sigma}_{11}(\boldsymbol{\omega}) + \widehat{\sigma}_{22}(\boldsymbol{\omega}) + (\widehat{\mu}_1(\boldsymbol{\omega}) - \widehat{\mu}_2(\boldsymbol{\omega}))^2)/d\varepsilon}{(\widehat{\sigma}_{11}(\boldsymbol{\omega}) + \widehat{\sigma}_{22}(\boldsymbol{\omega}) + (\widehat{\mu}_1(\boldsymbol{\omega}) - \widehat{\mu}_2(\boldsymbol{\omega}))^2)^2} \Big|_{\varepsilon=0} \\ &= \left( \frac{\widehat{\rho}_c(\boldsymbol{\omega})}{\widehat{\sigma}_{12}(\boldsymbol{\omega})} \alpha_{12}(\boldsymbol{\omega}) \right) \Big|_{\varepsilon=0} \\ &\quad - \left( \frac{\widehat{\rho}_c^2(\boldsymbol{\omega})}{2\widehat{\sigma}_{12}(\boldsymbol{\omega})} (\alpha_{11}(\boldsymbol{\omega}) + \alpha_{22}(\boldsymbol{\omega}) - 2(\beta_1(\boldsymbol{\omega}) - \beta_2(\boldsymbol{\omega}))) \right) \Big|_{\varepsilon=0} \\ &= \mathbf{h}^\top \frac{\widehat{\rho}_c}{n\widehat{\sigma}_{12}} \left( \mathbf{Z}_1 \odot \mathbf{Z}_2 - \widehat{\sigma}_{12} \mathbf{1}_n - \frac{\widehat{\rho}_c}{2} \mathbf{Z}_* \right) \end{aligned}$$

where  $\mathbf{Z}_* = (\mathbf{Z}_1 \odot \mathbf{Z}_1 - \widehat{\sigma}_{11} \mathbf{1}_n) + (\mathbf{Z}_2 \odot \mathbf{Z}_2 - \widehat{\sigma}_{22} \mathbf{1}_n) + 2(\widehat{\mu}_1 - \widehat{\mu}_2)(\mathbf{Z}_1 - \mathbf{Z}_2)$ .

To obtain the second derivative of the perturbed ML estimator of the CCC, we define

$$A(\boldsymbol{\omega}) = \frac{\hat{\rho}_c(\boldsymbol{\omega})}{\hat{\sigma}_{12}(\boldsymbol{\omega})} \alpha_{12}(\boldsymbol{\omega}), \quad B(\boldsymbol{\omega}) = \frac{\hat{\rho}_c^2(\boldsymbol{\omega})}{2\hat{\sigma}_{12}(\boldsymbol{\omega})} (\alpha_{11}(\boldsymbol{\omega}) + \alpha_{22}(\boldsymbol{\omega}) - 2(\beta_1(\boldsymbol{\omega}) - \beta_2(\boldsymbol{\omega}))).$$

Thus,

$$\frac{d^2 \rho_c(\boldsymbol{\omega})}{d\epsilon^2} \Big|_{\epsilon=0} = \frac{dA(\boldsymbol{\omega})}{d\epsilon} \Big|_{\epsilon=0} - \frac{dB(\boldsymbol{\omega})}{d\epsilon} \Big|_{\epsilon=0} = \mathbf{h}^\top (\boldsymbol{\Gamma}_1 - (\boldsymbol{\Gamma}_2 + \boldsymbol{\Gamma}_3)) \mathbf{h},$$

with

$$\begin{aligned} \boldsymbol{\Gamma}_1 &= \frac{2}{n^2} \frac{\hat{\rho}_c^2}{\hat{\sigma}_{12}} (\hat{\sigma}_{12} \mathbf{1}_n \mathbf{1}_n^\top - \mathbf{1}_n (\mathbf{Z}_1 \odot \mathbf{Z}_2)^\top - \mathbf{Z}_1 \mathbf{Z}_2^\top) - \frac{1}{2n^2} \left( \frac{\hat{\rho}_c}{\hat{\sigma}_{12}} \right)^2 ((\mathbf{Z}_1 \odot \mathbf{Z}_1 - \hat{\sigma}_{11} \mathbf{1}_n) \\ &\quad + (\mathbf{Z}_2 \odot \mathbf{Z}_2 - \hat{\sigma}_{22} \mathbf{1}_n) + 2(\hat{\mu}_1 - \hat{\mu}_2)(\mathbf{Z}_1 - \mathbf{Z}_2)) (\mathbf{Z}_1 \odot \mathbf{Z}_2 - \hat{\sigma}_{12} \mathbf{1}_n)^\top, \\ \boldsymbol{\Gamma}_2 &= \left( \frac{\nabla \hat{\rho}_c}{\hat{\sigma}_{12}} - \left( \frac{\hat{\rho}_c}{\hat{\sigma}_{12}} \right)^2 \frac{\mathbf{Z}_1 \odot \mathbf{Z}_2 - \hat{\sigma}_{12} \mathbf{1}_n}{n} \right) \left( \frac{\mathbf{Z}_1 \odot \mathbf{Z}_1 - \hat{\sigma}_{11} \mathbf{1}_n}{n} + \frac{\mathbf{Z}_2 \odot \mathbf{Z}_2 - \hat{\sigma}_{22} \mathbf{1}_n}{n} \right)^\top \\ &\quad + \frac{\hat{\rho}_c^2}{n^2 \hat{\sigma}_{12}} \left( \hat{\sigma}_{11}^2 \mathbf{1}_n \mathbf{1}_n^\top - \mathbf{1}_n (\mathbf{Z}_1 \odot \mathbf{Z}_1)^\top - \mathbf{Z}_1 \mathbf{Z}_1^\top + \hat{\sigma}_{22}^2 \mathbf{1}_n \mathbf{1}_n^\top - \mathbf{1}_n (\mathbf{Z}_2 \odot \mathbf{Z}_2)^\top - \mathbf{Z}_2 \mathbf{Z}_2^\top \right) \\ \boldsymbol{\Gamma}_3 &= \frac{\hat{\rho}_c^2}{n^2 \hat{\sigma}_{12}} ((\mathbf{Z}_1 - \mathbf{Z}_2)(\mathbf{Z}_1 - \mathbf{Z}_2)^\top - (n+1)(\hat{\mu}_1 - \hat{\mu}_2)(\mathbf{Z}_1 - \mathbf{Z}_2) \mathbf{1}_n^\top) \end{aligned}$$

where  $\hat{\rho}_c = \hat{\rho}_c(\boldsymbol{\omega})|_{\boldsymbol{\omega}=\boldsymbol{\omega}_0}$  and  $\hat{\mu}_1 = \hat{\mu}_1(\boldsymbol{\omega})|_{\boldsymbol{\omega}=\boldsymbol{\omega}_0}$ ,  $\hat{\mu}_2 = \hat{\mu}_2(\boldsymbol{\omega})|_{\boldsymbol{\omega}=\boldsymbol{\omega}_0}$ ,  $\hat{\sigma}_{11} = \hat{\sigma}_{11}(\boldsymbol{\omega})|_{\boldsymbol{\omega}=\boldsymbol{\omega}_0}$ ,  $\hat{\sigma}_{12} = \hat{\sigma}_{12}(\boldsymbol{\omega})|_{\boldsymbol{\omega}=\boldsymbol{\omega}_0}$ ,  $\hat{\sigma}_{22} = \hat{\sigma}_{22}(\boldsymbol{\omega})|_{\boldsymbol{\omega}=\boldsymbol{\omega}_0}$ . Finally, we have

$$\begin{aligned} \frac{\partial \hat{\rho}_c(\boldsymbol{\omega})}{\partial \boldsymbol{\omega}} \Big|_{\boldsymbol{\omega}=\boldsymbol{\omega}_0} &= \nabla_{\hat{\rho}_c} = \frac{\hat{\rho}_c}{n \hat{\sigma}_{12}} \left( \mathbf{Z}_1 \odot \mathbf{Z}_2 - \hat{\sigma}_{12} \mathbf{1}_n - \frac{\hat{\rho}_c}{2} \mathbf{Z}_* \right) \\ \frac{\partial^2 \hat{\rho}_c(\boldsymbol{\omega})}{\partial \boldsymbol{\omega} \partial \boldsymbol{\omega}^\top} \Big|_{\boldsymbol{\omega}=\boldsymbol{\omega}_0} &= \mathbf{H}_{\hat{\rho}_c} = \boldsymbol{\Gamma}_1 - (\boldsymbol{\Gamma}_2 + \boldsymbol{\Gamma}_3), \end{aligned}$$

this yields Equations (19) and (20).

### Appendix C: Proof of Equations (21) and (23)

For the perturbed estimator of the probability of agreement, defined in Equation (16), we have that

$$\frac{d \hat{\psi}_c(\boldsymbol{\omega})}{d\epsilon} \Big|_{\epsilon=0} = \sum_{i=1}^n \frac{\partial \hat{\psi}_c(\boldsymbol{\omega})}{\partial \omega_i} \frac{d\omega_i}{d\epsilon} \Big|_{\epsilon=0} = \mathbf{h}^\top \nabla_{\hat{\psi}_c},$$

where  $\nabla_{\hat{\psi}_c} = \partial \hat{\psi}_c(\boldsymbol{\omega}) / \partial \boldsymbol{\omega} |_{\boldsymbol{\omega}=\boldsymbol{\omega}_0}$ , with  $\boldsymbol{\omega}_0 = \mathbf{1}$  a  $n$ -dimensional vector of ones. Thus, the  $i$ th element of vector  $\nabla_{\hat{\psi}_c}$  assumes the form.

$$\frac{\partial \hat{\psi}_c(\boldsymbol{\omega})}{\partial \omega_i} = 2\phi \left( \frac{c - \hat{\mu}_D(\boldsymbol{\omega})}{\hat{\sigma}_D(\boldsymbol{\omega})} \right) \frac{\partial}{\partial \omega_i} \left( \frac{c - \hat{\mu}_D(\boldsymbol{\omega})}{\hat{\sigma}_D(\boldsymbol{\omega})} \right), \quad i = 1, \dots, n.$$

In fact, it is easy to see that

$$\frac{\partial}{\partial \omega_i} \left( \frac{c - \hat{\mu}_D(\boldsymbol{\omega})}{\hat{\sigma}_D(\boldsymbol{\omega})} \right) = -\frac{1}{\hat{\sigma}_D^2(\boldsymbol{\omega})} \left\{ \hat{\sigma}_D(\boldsymbol{\omega}) \frac{\partial \hat{\mu}_D(\boldsymbol{\omega})}{\partial \omega_i} + (c - \hat{\mu}_D(\boldsymbol{\omega})) \frac{\partial \hat{\sigma}_D(\boldsymbol{\omega})}{\partial \omega_i} \right\},$$

simple calculations lead to the aforementioned derivative, evaluated at  $\omega = \omega_0$  can be written as

$$\frac{\partial}{\partial \omega_i} \left( \frac{c - \hat{\mu}_D(\omega)}{\hat{\sigma}_D(\omega)} \right) \Big|_{\omega=\omega_0} = -\frac{1}{n\hat{\sigma}_D^2} \left[ \hat{\sigma}_D(Z_{i1} - Z_{i2}) + \frac{1}{2} \left( \frac{c - \hat{\mu}_D}{\hat{\sigma}_D} \right) \left\{ \frac{n-2}{n} (Z_{i1} - Z_{i2})^2 - \hat{\sigma}_D^2 \right\} \right],$$

which can be written in compact form as

$$\frac{\partial}{\partial \omega} \left( \frac{c - \hat{\mu}_D(\omega)}{\hat{\sigma}_D(\omega)} \right) \Big|_{\omega=\omega_0} = -\frac{1}{n\hat{\sigma}_D} \mathbf{s},$$

with  $\mathbf{s}$  being defined in Equation (22) and the Equation (21) is verified.

Tedious but simple calculations lead to

$$\frac{\partial^2 \hat{\psi}_c(\omega)}{\partial \omega \partial \omega^\top} = 2\phi \left( \frac{c - \hat{\mu}_D(\omega)}{\hat{\sigma}_D(\omega)} \right) \left\{ \frac{\partial^2}{\partial \omega \partial \omega^\top} \left( \frac{c - \hat{\mu}_D(\omega)}{\hat{\sigma}_D(\omega)} \right) - \left( \frac{c - \hat{\mu}_D(\omega)}{\hat{\sigma}_D(\omega)} \right) \frac{\partial}{\partial \omega} \left( \frac{c - \hat{\mu}_D(\omega)}{\hat{\sigma}_D(\omega)} \right) \frac{\partial}{\partial \omega^\top} \left( \frac{c - \hat{\mu}_D(\omega)}{\hat{\sigma}_D(\omega)} \right) \right\},$$

for  $i, j = 1, \dots, n$ . Moreover

$$\begin{aligned} \frac{\partial^2}{\partial \omega \partial \omega^\top} \left( \frac{c - \hat{\mu}_D(\omega)}{\hat{\sigma}_D(\omega)} \right) &= \frac{1}{\hat{\sigma}_D^4(\omega)} \frac{\partial \hat{\sigma}_D^2(\omega)}{\partial \omega} \left\{ \hat{\sigma}_D(\omega) \frac{\partial \hat{\mu}_D(\omega)}{\partial \omega^\top} + (c - \hat{\mu}_D(\omega)) \frac{\partial \hat{\sigma}_D(\omega)}{\partial \omega^\top} \right\} \\ &- \frac{1}{\hat{\sigma}_D^2(\omega)} \left\{ \frac{\partial \hat{\sigma}_D(\omega)}{\partial \omega} \frac{\partial \hat{\mu}_D(\omega)}{\partial \omega^\top} - \frac{\partial \hat{\mu}_D(\omega)}{\partial \omega} \frac{\partial \hat{\sigma}_D(\omega)}{\partial \omega^\top} + \hat{\sigma}_D(\omega) \frac{\partial^2 \hat{\mu}_D(\omega)}{\partial \omega \partial \omega^\top} + (c - \hat{\mu}_D(\omega)) \frac{\partial^2 \hat{\sigma}_D(\omega)}{\partial \omega \partial \omega^\top} \right\}, \end{aligned}$$

noticing that  $\partial \hat{\mu}_D(\omega)/\partial \omega$  and  $\partial \hat{\sigma}_D(\omega)/\partial \omega$  were previously calculated in order to obtain  $\nabla_{\hat{\psi}_c}$ , it follows that it is only required to compute  $\partial^2 \hat{\mu}_D(\omega)/\partial \omega \partial \omega^\top$  and  $\partial^2 \hat{\sigma}_D(\omega)/\partial \omega \partial \omega^\top$ . Thus, evaluating in the null perturbation vector follows that its  $(i, j)$ th is given by

$$\begin{aligned} \frac{\partial^2 \hat{\mu}_D(\omega)}{\partial \omega_i \partial \omega_j} \Big|_{\omega=\omega_0} &= -\frac{1}{n} \{ (Z_{i1} - Z_{i2}) + (Z_{j1} - Z_{j2}) \} \\ \frac{\partial^2 \hat{\sigma}_D(\omega)}{\partial \omega_i \partial \omega_j} \Big|_{\omega=\omega_0} &= \frac{1}{n^2} \left[ 2(Z_{j1} - Z_{j2})^2 - \left\{ \frac{n-2}{n} (Z_{i1} - Z_{i2})^2 - \hat{\sigma}_D^2 \right\} - \left\{ \frac{n-2}{n} (Z_{j1} - Z_{j2})^2 - \hat{\sigma}_D^2 \right\} \right], \end{aligned}$$

for  $i, j = 1, \dots, n$ . Bringing together all the above elements we obtain  $\mathbf{H}_{\hat{\psi}_c}$  and Equation (23) is proved.

### References

Anderson, T.W. (2003). *An Introduction to Multivariate Statistical Analysis, 3rd Edition*. Wiley, New York.

Cadigan, N., Farrel, P. (2002). Generalized local influence with applications to fish stock cohort analysis. *Applied Statistics* 51, 469–483.

Carstensen, B. (2010). *Comparing Clinical Measurement Methods*. Wiley, Chichester.

Chen, F., Zhu, H., Lee, S. (2009). Perturbation selection and local influence analysis for nonlinear structural equation model. *Psychometrika* 74, 493–516.

Choudhary, P., Nagaraja, H. (2017). *Measuring Agreement, Models, Methods, and Applications*. Wiley, New York.

Cook, R.D. (1986). Assessment of local influence (with discussion). *Journal of the Royal Statistical Society, Series B* 48, 133–169.

Feng, D., Baumgartner, R., Svetnik, V. (2015). A robust bayesian estimate of the concordance correlation coefficient. *Journal of Biopharmaceutical Statistics* 25, 490–507.

Fung, W.K., Kwan, C. (1997). A note on local influence based on normal curvature. *Journal of the Royal Statistical Society, Series B* 59, 839–843.

Galea, M., Giménez, P. (2016). Local influence diagnostics for the test of mean-variance efficiency and systematic risks in the capital asset pricing model. *Statistical Papers* 60, 293–312.

- Giménez, P., Galea, M. (2013). Influence measures on corrected score estimators in functional heteroscedastic measurement error models. *Journal of Multivariate Analysis* **114**, 1–15.
- Hiriote, S., Chinchilli, V.M. (2011). Matrix-based concordance correlation coefficient for repeated measures. *Biometrics* **67**, 1007–1016.
- Lawrance, A. (1988). Regression transformation diagnostics using local influence. *Journal of the American Statistical Association* **83**, 1067–1072.
- Lin, L. (1989). A concordance correlation coefficient to evaluate reproducibility. *Biometrics* **45**, 225–268.
- Lin, L., Hedayat, A.S., Wu, W. (2011). *Statistical Tools for Measuring Agreement*. Springer, New York.
- Magnus, J., Neudecker, H. (2007). *Matrix Differential Calculus with Applications in Statistics and Econometrics, 3rd Edition*. Wiley, New York.
- McBride, G.B. (2005). A proposal for strength-of-agreement criteria for Lin's concordance correlation coefficient. *NIWA Client Report: HAM 2005-062*. National Institute of Water & Atmospheric Research, Ltd. Hamilton, New Zealand.
- Poon, W., Poon, Y. (1999). Conformal normal curvature and assessment of local influence. *Journal of the Royal Statistical Society, Series B* **61**, 51–61.
- Shi, X., Zhu, H., Ibrahim, J.G. (2009). Local influence for generalized linear models with missing covariates. *Biometrics* **65**, 1164–1174.
- Stevens, N.T., Steiner, S.H., MacKay, R.J. (2017). Assessing agreement between two measurement systems: An alternative to the limits of agreement approach. *Statistical Methods in Medical Research* **26**, 2487–2504.
- Svetnik, V., Ma, J., Soper, K.A., Doran, S., Renger, J.J., Deacon, S., Koblan, K.S. (2007). Evaluation of automated and semi-automated scoring of polysomnographic recordings from a clinical trial using zolpidem in the treatment of insomnia. *SLEEP* **30**, 1562–1574.
- Thomas, W., Cook, R.D. (1990). Assessing influence on predictions from generalized linear models. *Technometrics* **32**, 59–65.
- Wu, X., Luo, Z. (1993). Second, order approach to local influence. *Journal of the Royal Statistical Society, Series B* **55**, 929–936.
- Zhu, H., Ibrahim, J.G., Lee, S., Zhang, H. (2007). Perturbation selection and influence measures in local influence analysis. *The Annals of Statistics* **35**, 2565–2588.